Available online at www.sciencedirect.com
ScienceDirect
Trans. Nonferrous Met. Soc. China 32(2022) 4076−4087
Transactions of Nonferrous Metals Society of China
www.tnmsc.cn

Structure−activity relationships of oxime compounds as flotation collectors by DFT calculations

Yu-xi LU, Shuai WANG, Zhan-fang CAO, Xin MA, Hong ZHONG

Hunan Provincial Key Laboratory of Efficient and Clean Utilization of Manganese Resources, School of Chemistry and Chemical Engineering, Central South University, Changsha 410083, China

Received 26 September 2021; accepted 31 May 2022

Abstract: The relationships between the structure of oxime compounds (R^1R^2C═NOH, R^1/R^2=alkyl groups) with different substituents and their corresponding flotation performances were studied. The analyses of density functional theory (DFT) calculations illustrated that the introduced phenyl group at the R^1 position could enhance the acidity, while the heptyl group could effectively increase the hydrophobicity and benefit van der Waals interactions. Meanwhile, the introduced amino group at the R^2 position could provide cationic sites to interact with negatively charged surfaces of minerals, while the introduced hydroxyl group could provide additional action sites to form stable chelates with metal ions. Based on the structure−activity relationships, structural optimization was carried out to obtain three efficient collectors, which possessed superior flotation separation performances, proving the effectiveness of the structural modification to oxime compounds in this work.

Key words: oxime compounds; flotation collector; DFT calculations; structure–reactivity relationship; structural modification

1 Introduction

Froth flotation, a beneficiation process of purifying and enriching minerals from pulp according to the differences in surface properties, has been widely employed in the mineral processing industry. During the flotation process, the collector is particularly important for the flotation process and a variety of collectors with different functional groups have been developed in recent years [1,2].

Oximes refer to the organic compounds formed by the interaction of hydroxylamine and aldehydes or ketones containing carbonyl groups [3] and can be expressed as R^1R^2C═NOH. Owing to the lone pair electrons of N and O atoms, oxime compounds possess strong chelating ability with metal ions such as Cu, Fe, U, Pd and Ni [4,5]. In the field of flotation collectors, oxime derivatives also play an important role. Benzohydroxamic acid (BHA) has been proven to be an effective collector for refractory minerals such as smithsonite, wolframite, scheelite and cassiterite [6−9]. In addition, salicylaldoxime has been reported as an effective collector for copper oxide (malachite) ore [10]. Therefore, studying the properties of oxime compounds substituted by different functional groups is of great value for their application in the field of collectors.

In view of the long-term research on the development of new high-efficiency flotation collectors, the investigation of structure−activity relationship has been proven to possess strong guiding value for designing effective collectors [11]. Herein, to expound the structures and properties of oxime compounds, DFT calculations are introduced. In recent decades, due to its sufficient accuracy and

Corresponding author: Xin MA, E-mail: maxin2013@csu.edu.cn; Hong ZHONG, E-mail: zhongh@csu.edu.cn
DOI: 10.1016/S1003-6326(22)66079-5

low cost in reproducing the experimental values of molecular geometry, charge and thermodynamic properties, density functional theory (DFT) has become a common method for calculating the physical and chemical properties of chemical species and biomolecules [12]. The quantum chemical properties of collectors could be obtained by DFT calculations, and then their flotation performances could be analyzed from these properties. Flotation experiments are used to verify the flotation performances concluded by DFT calculations, which is an area that the present work seeks to address by exploring the structure−activity relationship of oxime compounds with different substituent groups via DFT calculations and flotation tests.

In this work, we substituted the R^1 and R^2 groups of oxime compounds ($R^1R^2C{=}NOH$) with different functional groups, where R^1 was the phenyl (Ph) and heptyl (C_7H_{15}) groups, respectively, and R^2 was the hydrogen atom (H), hydroxyl (—OH), and amino ($—NH_2$) groups, respectively. The molecular characterizations of these oxime compounds were investigated through DFT calculations, and the corresponding flotation performances were summarized by the relevant study. Therefore, the relationships between collector structures and flotation performances were established. Based on the obtained structure−activity relationship, we modified the structure of aldoxime, hydroxime and amidoxime compounds and verified their flotation performances through flotation tests, which provided a theoretical and experimental basis for the development of new effective flotation collectors.

2 Experimental

2.1 Computational calculation methods

As shown in Fig. 1, substances from ① to ⑨ were oxime compounds requiring DFT calculations. Meanwhile, to explain the differences in chemical properties between the oxime group and hydroxylamine, we selected their simplest molecules for comparison, namely methyl hydroxylamine (MHA) and formaldoxime (FAO).

At the beginning of DFT calculations, the initial structures of the above compounds were firstly drawn in the ChemBioDraw module of ChemBioOffice 2014 software. Then, the structures were optimized in Gaussian 09W software by using the semi-empirical/PM3 method and the optimized structures were continuously optimized by the DFT method at the B3LYP/6-311+G(d) level. Finally, the properties of the optimized molecules were calculated under the same basis set. To obtain their geometric configurations and electronic properties in aqueous solution, the polarizable continuum

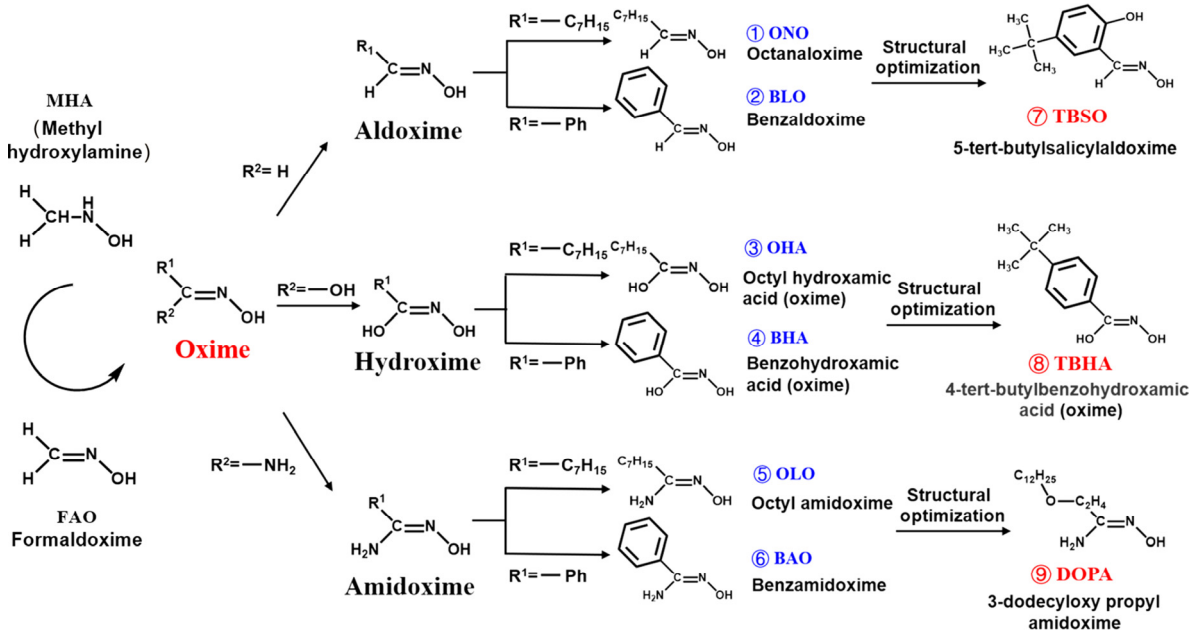

Fig. 1 Molecular design route of oxime compounds (—Ph= phenyl group)

model (IEF-PCM) was introduced into the calculations with water as the solvent.

To study the solution chemistry of the oxime compounds, the parameters lg *P* and pK_a were calculated by Advanced Chemistry Development (ACD/Labs) software. The value of lg *P* referred to the distribution of substances in the oil−water two-phase, while a larger lg *P* value indicated stronger lipophilicity and hydrophobicity [13]. In addition, pK_a referred to the dissociation constant which reflected the strength of acid, while a lower pK_a value generally referred to stronger acidity [14].

2.2 Materials and reagents

The cassiterite and quartz samples employed in the micro-flotation tests were obtained from Sichuan and Yunnan Provinces in China with 95.51% and 99.29% purity, respectively. The mineral samples were manually ground to sizes from 38 to 76 μm. In addition, the cassiterite ore samples for the bench-scale flotation tests were obtained from Dulong Mine of Yunnan Province in China with 0.17% Sn, while the main gangue minerals included pyrite, quartz, calcite and other sulfide minerals.

All the reagents used in the experiments were of analytical purity, while distilled water was used in all tests.

2.3 Flotation tests

The micro-flotation tests were conducted in an XFGCII flotation machine with an impeller speed of l650 r/min. As shown in Fig. 2(a), 2.0 g of mineral sample was placed into a plexiglass cell (30 mL) and filled with a specific amount of water for 2 min. Then, hydrochloric acid or sodium hydroxide solution was added to adjust the pH. After stirring for 2 min, the collector and frother (methyl isobutyl carbinol, MIBC) were successively added into the pulp. However, MIBC was only employed in the micro-flotation test by using BHA as the collector, while the concentration of MIBC was 15 mg/L. The flotation tests were conducted for 4 min, after which the concentrates and tails were separated and dried to calculate the flotation recovery.

The bench-scale flotation tests were carried out in a self-aeration XFD−63 machine, while the volume for rougher and cleaner flotation was 1.5 and 0.5 L, respectively. The specific flowsheet of the locked cycle flotation tests is exhibited in Fig. 2(b). In addition, 600 g ores were used in rougher flotation and the impeller speed was fixed at l650 r/min.

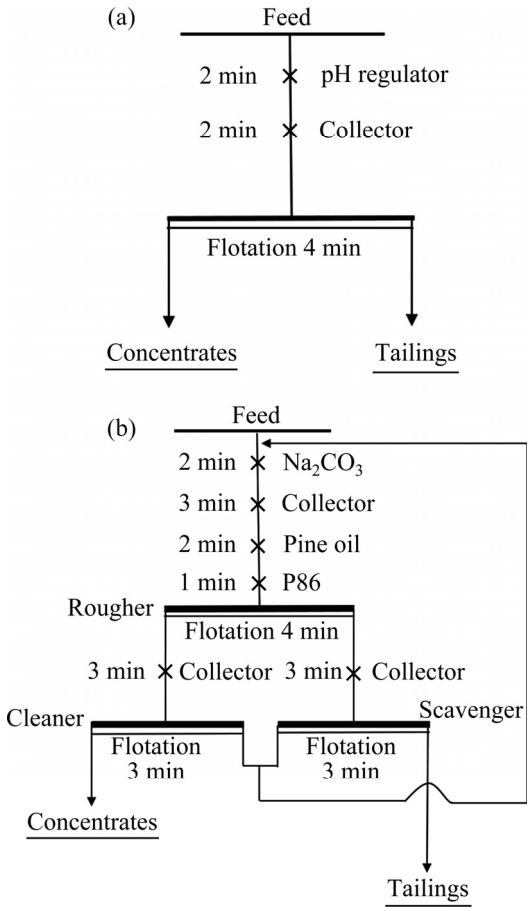

Fig. 2 Flow charts of micro-flotation (a) and bench-scale flotation (b) tests

3 Results and discussion

3.1 Energy and physicochemical properties

After the computational calculations, the selected optimized geometrical parameters of the oxime compounds are exhibited in Table 1, while their schematic representation is presented in Fig. 3. MHA, octyl amidoxime (OLO), benzamidoxime (BAO) and 3-dodecyloxy propyl amidoxime (DOPA) existed in the form of cations, which was mainly because the N atom with lone pair electrons possessed a strong ability to obtain electrons and increased the alkalinity of molecules. In Table 1, the dipole moment can be considered as a parameter to assess the van der Waals and electro-static interactions between collectors and metal ions, while larger value of dipole moment generally

Table 1 Selected optimized geometrical parameters

Species		lg *P*	pK_a	Dipole moment/D	E_{HOMO}/eV	E_{LUMO}/eV	ΔE/eV	τ for (A5−C4−N3−O2)/(°)	E_t/eV
MHA	Cation	−1.10	5.96 (pK_{a1}) 14.00 (pK_{a2})	3.131	−10.331	−0.666	9.665	55.589	−4667.085
	Molecule	−1.10		1.021	−7.022	0.171	7.193	51.500	−4655.289
	Anion	−1.10		6.696	−3.924	0.425	4.349	50.949	−4641.623
FAO	Molecule	−1.28	11.10	0.521	−7.802	−0.835	6.967	0.034	−4622.290
	Anion	−1.28		4.412	−4.690	0.316	5.006	−0.081	−4609.202
ONO	Molecule	3.030	11.92	1.332	−7.354	−0.345	7.009	0	−12112.445
	Anion	3.030		23.966	−4.522	0.324	4.846	0	−12099.163
BLO	Molecule	1.765	11.37	1.281	−6.685	−1.724	4.961	0	−10911.111
	Anion	1.765		14.126	−4.818	−0.843	3.975	0	−10898.088
OHA	Molecule	1.540	10.00	3.689	−6.883	−0.108	6.775	−0.001	−14160.161
	Anion	1.540		24.733	−4.435	0.131	4.566	0.001	−14146.775
BHA	Molecule	0.275	9.01	3.716	−6.580	−1.553	5.027	0	−12958.641
	Anion	0.137		17.746	−7.324	1.842	9.166	0	−12867.412
OLO	Cation	2.763	6.69 (pK_{a1}) 12.94 (pK_{a2})	19.335	−8.402	−1.319	7.083	0.525	−13631.041
	Molecule	2.763		2.717	−6.201	0.009	6.210	0.002	−13619.594
	Anion	2.121		22.590	−4.167	0.216	4.383	0.002	−13606.078
BAO	Cation	1.024	4.53 (pK_{a1}) 11.40 (pK_{a2})	9.138	−7.327	−2.395	4.932	0.359	−12429.504
	Molecule	1.024		2.441	−6.330	−1.226	5.104	−4.658	−12418.176
	Anion	1.024		13.671	−4.530	−0.728	3.802	−4.215	−12404.971
TBSO	Molecule	2.924	11.91	3.599	−6.242	−1.677	4.565	0.001	−17238.530
	Anion	1.725		20.090	−4.770	−0.811	3.959	0.003	−17225.449
TBHA	Molecule	2.101	9.04	4.623	−6.560	−1.326	5.234	−2.929	−17238.624
	Anion	1.963		23.964	−4.653	−0.697	3.956	−2.191	−17225.430
DOPA	Cation	5.334	5.69 (pK_{a1}) 12.55 (pK_{a2})	39.383	−7.364	−1.428	5.936	−0.388	−23168.013
	Molecule	5.334		1.133	−6.388	−0.010	6.378	2.679	−23156.623
	Anion	4.859		38.275	−4.442	0.196	4.638	3.622	−23143.240

A5 stands for the atom in R^2 connected to C4 (Fig. 3). pK_a stands for the dissociation constant of the oxime compound, while pK_{a1} and pK_{a2} stand for the first and second dissociation constants, respectively

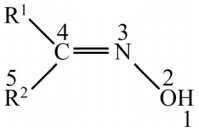

Fig. 3 Schematic representation of oxime compounds

means stronger interactions to some extent [12,15]. The highest occupied molecular orbital (HOMO) and lowest unoccupied molecular orbital (LUMO) can be used to evaluate the electron donating and accepting ability of a collector, respectively [16]. The energy gap (ΔE) between the HOMO and LUMO ($\Delta E=E_{LUMO}-E_{HOMO}$) can be used as a stability index for evaluating the chemical activity of a collector, while a lower value of ΔE indicates higher chemical reactivity and lower stability [16,17]. τ is the dihedral angle, and E_t represents the total energy.

In the oxime compounds, the lg *P* and dipole moment values of oxime compounds with R^1=—C_7H_{15} were significantly higher than those with R^1=—Ph, suggesting that compared to the phenyl group, the heptyl group could effectively enhance the hydrophobicity and van der Waals interaction of the collector, which benefited its collecting property in flotation. However, the pK_a values of oxime compounds with R^1=—C_7H_{15} were less than those with R^1=—Ph, revealing their weaker acidity. Compared with the heptyl group, the conjugation and inductive effects of the phenyl group are generally embodied in the electron

receptor effect, which makes the electron cloud on the connected group more inclined to the phenyl group. In this way, the attraction to the positively charged hydrogen atom is weakened; thus, the hydrogen atom on the hydroxyl group is easier to ionize, resulting in greater acidity of the oxime compounds with R^1=—Ph. Notably, the dihedral angles of A5−C4−N3−O2 of several oxime compounds were very small, basically less than 1°, revealing that the four atoms of the oxime group were basically in the same plane, which was conducive to the formation of conjugated π bonds [13,18]. When the oxime compounds interact with the metal ions on the mineral surfaces, the oxygen and nitrogen atoms with lone pair electrons could provide electrons to the empty orbit of the metal ions to form coordination bonds, so as to form a stable complex [19,20]. Therefore, the configuration of oxime compounds could not only improve the interaction ability with mineral metal ions, but also help to form a more stable chelating ring after interacting with metal ions.

3.2 Charge population

The values of selected atomic charges for oxime compounds based on Mulliken and natural atomic charges are listed in Table 2, while their molecular electrostatic potential (MEP) maps are exhibited in Fig. 4. Molecular electrostatic potential plays a unique role in understanding the interaction and reaction sites between molecules, and its related color gradient map (MEP map) is widely

Table 2 Selected atomic charges

Species		Mulliken charge/eV					Natural charge/eV				
		H1	O2	N3	C4	A5	H1	O2	N3	C4	A5
MHA	Cation	11.570	−4.686	−14.785	−17.619	8.318	13.585	−13.941	−5.930	−9.897	6.247
	Molecule	10.855	−10.612	−12.029	−18.266	6.714	12.890	−17.023	−10.359	−10.202	5.141
	Anion	−	−22.723	−10.207	−19.248	5.955	−	−26.072	−12.116	−10.258	4.522
FAO	Molecule	11.120	−9.503	−3.965	−11.607	6.676	13.136	−15.952	−4.587	−2.853	4.893
	Anion	−	−17.739	−3.934	−15.981	4.838	−	−21.567	−5.514	−8.101	3.533
ONO	Molecule	10.965	−5.331	−10.384	−4.770	6.415	13.053	−16.170	−5.440	2.638	4.968
	Anion	−	−14.939	−10.281	−1.841	4.526	−	−22.551	−6.001	−1.342	3.527
BLO	Molecule	11.065	−4.728	−9.518	−18.678	6.454	13.164	−15.638	−4.653	1.631	5.236
	Anion	−	−12.420	−9.005	−14.532	4.692	−	−20.165	−4.439	−2.064	4.009
OHA	Molecule	10.924	−4.973	−14.062	2.232	−10.339	13.024	−16.143	−7.323	14.715	−18.671
	Anion	−	−15.456	−13.642	5.326	−12.230	−	−23.189	−7.862	11.813	−20.155
BHA	Molecule	11.232	−3.701	−14.918	−9.698	−8.769	13.121	−15.631	−6.625	14.064	−18.324
	Anion	−	−13.997	−16.736	−2.687	−13.674	−	−23.992	−6.220	13.019	−20.733
OLO	Cation	11.842	−3.630	−11.092	2.862	−18.219	13.83	−15.543	−3.543	11.099	−19.068
	Molecule	10.869	−6.279	−15.809	8.296	−20.611	13.099	−17.268	−8.438	11.029	−21.773
	Anion	−	−17.094	−14.890	9.439	−20.994	−	−24.353	−9.181	8.768	−23.619
BAO	Cation	11.946	−4.026	−9.097	−11.666	−21.596	13.957	−15.249	−3.097	10.366	−19.046
	Molecule	10.889	−8.183	−10.022	−9.847	−17.533	13.215	−16.812	−7.413	10.367	−21.631
	Anion	−	−15.344	−9.839	−8.870	−17.908	−	−21.701	−6.695	7.419	−23.522
TBSO	Molecule	10.908	−4.156	−10.498	−3.661	6.554	13.126	−15.776	−4.850	1.563	5.552
	Anion	−	−11.984	−9.722	3.055	4.859	−	−20.304	−4.522	−2.755	4.390
TBHA	Molecule	11.037	−6.101	−11.075	−8.846	−8.913	13.091	−15.829	−6.725	14.088	−18.441
	Anion	−	−13.696	−11.845	−1.159	−11.376	−	−21.155	−6.354	10.800	−19.889
DOPA	Cation	11.899	−4.514	−9.620	−1.126	−18.467	13.876	−15.436	−3.426	10.970	−19.041
	Molecule	10.928	−6.976	−13.764	1.983	−17.109	13.147	−17.047	−8.064	11.013	−21.797
	Anion	−	−17.369	−11.807	1.068	−17.972	−	−23.640	−8.255	8.477	−23.632

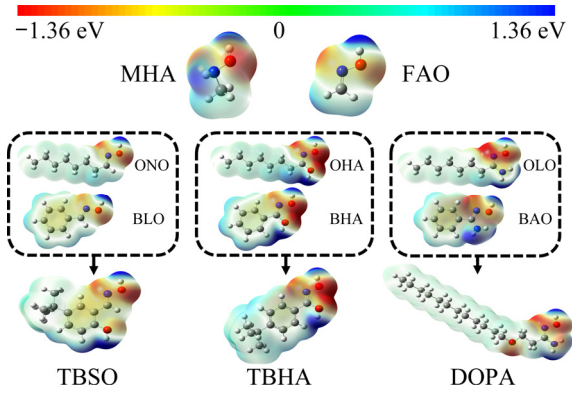

Fig. 4 MEP maps for oxime compounds

considered as an effective tool for analyzing molecular functional sites and predicting their interactions [21]. In MEP maps, red and blue areas represent the most negative and positive electrostatic potential regions, respectively. As shown in Table 2, the nitrogen and oxygen atoms of all these oxime compounds were obviously negatively charged, while the charges of nitrogen and oxygen atoms of oxime compounds with R^1=—Ph were basically lower than those with R^1=—C_7H_{15}, which was mainly due to better electron donating ability of the nonpolar carbon chain.

The distribution of charges in the whole molecule can be observed intuitively from the MEP map. In Fig. 4, the negative charges of oxime compounds were mainly concentrated on the oxygen and nitrogen atoms of the oxime groups, revealing the electron-donating ability of the oxime group. Unlike octanaloxime (ONO) and benzaldoxime (BLO), the red regions in octyl hydroxamic acid (OHA) and benzohydroxamic acid (BHA) were relatively large because the oxygen atoms in the hydroxyl groups introduced at the R^2 substituent groups possessed strong negative charges. Therefore, the negative charges of OHA and BHA were mainly distributed on the two oxygen atoms of the hydroxime group, while their unique spatial structures made it easier for these two oxygen atoms to interact with metal ions on the mineral surfaces, so as to form five-membered ring complexes [22,23]. It was noteworthy that due to the introduction of amino groups at R^2 substituent groups, OLO and BAO could exhibit a certain cationic nature. Under acidic and neutral conditions, OLO and BAO exist in cationic form, thus they can be adsorbed on negatively charged mineral surfaces. Studies [24,25] have shown that the tungsten bearing minerals, such as wolframite and scheelite, are negatively charged in most instances. Therefore, OLO and BAO can realize the electrostatic adsorption on wolframite or scheelite surfaces, which show the potential to become the collectors for tungsten ores.

3.3 Overall effect

To better evaluate the influence of substituent groups on oxime compounds, the key parameters related to their physicochemical properties were summarized and are listed in Table 3. This result revealed that nonpolar carbon chains (heptyl groups) could effectively increase the hydrophobicity of the collector and benefit van der Waals interactions between the collector and mineral surfaces. The introduction of hydroxyl groups could improve acidity and provide additional action sites to form stable chelates with metal ions. Therefore, the hydroxylamine compounds OHA and BHA should be considered as valuable collectors for oxide minerals with active metal sites on surfaces such as malachite, cassiterite and hematite [20,26,27]. In

Table 3 Physicochemical properties of ONO, BLO, OHA, BHA, OLO and BAO

Parameter	Property	Order					
		ONO	BLO	OHA	BHA	OLO	BAO
lg *P*	Hydrophobicity	1	3	4	6	2	5
pK_a	Acid−base properties	4	3	2	1	6	5
Dipole moment	van der Waals interaction	2	5	1	4	3	6
ΔE	Chemical activity	3	1	2	6	5	4
τ	Formation of conjugate π bond	1	1	4	1	6	5

The results are listed in descending order (1>2>3>4>5>6). For the parameter of pK_a, order 1 stands for the strongest acidity, while order 6 stands for the weakest

addition, the aldoxime compound with R^1=—C_7H_{15} (ONO) may also be used as a practicable collector in flotation. The introduced amino groups of amidoxime compounds could improve alkalinity and possess strong chemical activity, and also provide cationic sites to interact with negatively charged minerals. Thus, the amidoxime compounds OLO and BAO should be considered as possible collectors for tungsten ores which were negatively charged in most instances. However, the surfaces of common gangue mineral quartz are also negatively charged, which are easy to interact with cationic collector through electrostatic attraction. Due to the strong cationic nature, OLO should possess certain collection ability for quartz; hence, its application in flotation separation might be limited.

The applications of oxime compounds in flotation are shown in Table 4. Noticeably, BHA, OHA and ONO were proven to be available collectors in flotation, while BLO, OLO and BAO were rarely used in flotation due to their unsatisfactory performances, which were basically consistent with the conclusions of our previous evaluations. Based on the above analyses, we obtained a summary of the characteristics of the oxime compounds, as shown in Fig. 5. It was clear

Table 4 Applications of ONO, BLO, OHA, BHA, OLO and BAO in flotation

Collector		Application in flotation
Aldoxime	ONO	ONO possessed strong collecting ability to malachite, and also a certain collecting ability to chalcopyrite, chalcocite and pyrite [28]
	BLO	No relevant research was reported on the application of BLO in flotation
Hydroxime	OHA	Due to its strong collecting ability, OHA was studied in the flotation of cassiterite, malachite, wolframite and other minerals [29−31]
	BHA	Due to its excellent solubility and selectivity, BHA was widely studied and used in the flotation of wolframite, scheelite, ilmenite, cassiterite and other oxidized ores [8,32−34]
Amidoxime	OLO	The flotation performance of OLO to malachite good not well enough [20]
	BAO	No relevant research has been reported on the flotation performance of BAO, while methyl benzamide oxime (MBO), with a methyl group added to the phenyl group of BAO, possessed a certain collecting ability to wolframite [35]

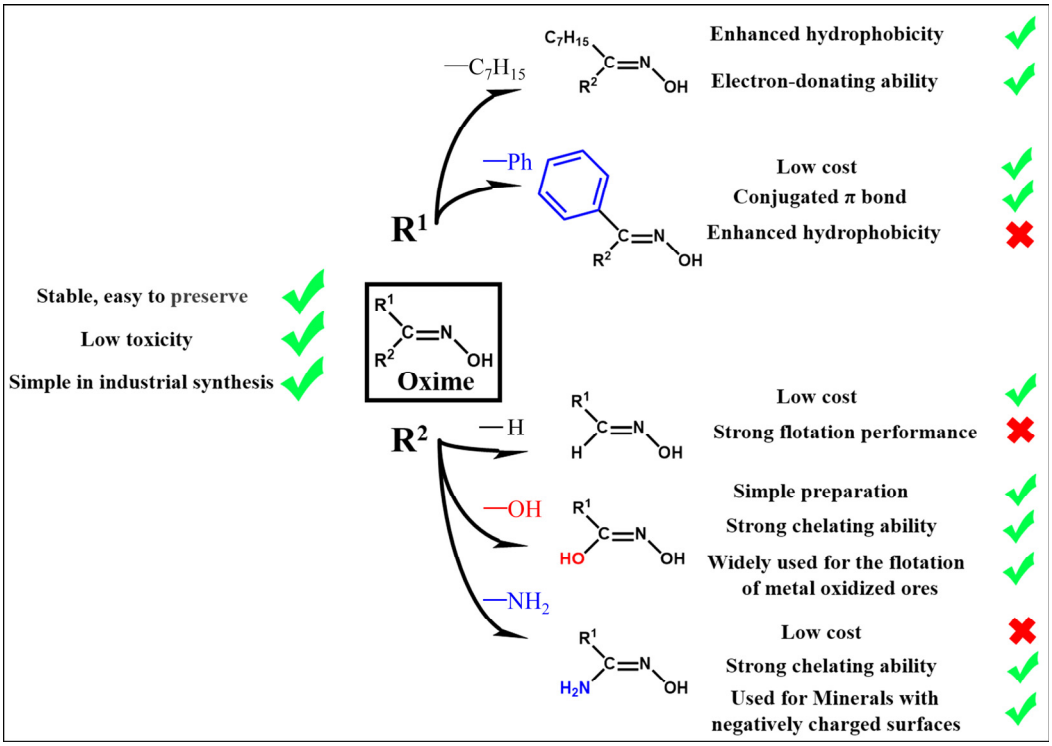

Fig. 5 Summary of characteristics of oxime compounds

that for the R^1 substituent group, the heptyl group could enhance hydrophobicity and electron-donating ability, but its strong hydrophobicity and foaming ability weakened the selectivity, which limited its application in flotation. Unlike heptyl groups, phenyl groups are often low cost and can provide conjugated π bonds, but they cannot provide enough hydrophobicity for oxime compounds, which is why BHA is employed with metal ion activators such as lead ions, causing environmental hazards. For the R^2 position substituent group, hydroxylamine compounds had simple preparation and strong chelating ability and were widely used in flotation, but the defects of the R^1 substituent group limited their application. In addition, amidoxime and aldoxime compounds possessed relative merits and weaknesses, which require further optimization.

3.4 Optimization of flotation performance

To improve the flotation performances of oxime compounds, structural modification of the substituent groups was employed in this work, and the designed flowchart is exhibited in Fig. 6. For the aldoxime compound, to enhance the hydrophobicity, a tert-butyl group was introduced to the R^1 substituent group on the basis of the phenyl group. The unique umbrella-shaped structure of the tert-butyl group was conducive to enhancing the dispersion characteristic of the collector in water [36,37]. After that, a hydroxyl group was introduced to provide an additional action site, while 5-tert-butylsalicylaldoxime (TBSO) was designed. Due to its strong chelating ability, the hydroxylamine compound was only necessary to enhance the hydrophobicity of the R^1 substituent group, while 4-tert-butylbenzohydroxamic acid (TBHA) was designed. For the amidoxime compound, an undecyl group was introduced to enhance the hydrophobicity but resulted in a high production cost. To reduce the cost, dodecyloxy ethyl was selected as the R^1 substituent group, thus 3-dodecyloxy propyl amidoxime (DOPA) was designed [38].

Compared with ONO and BLO, TBSO possessed stronger chemical activity, acidity and van der Waals interactions. Meanwhile, on the premise of maintaining the negative charges of N and O atoms on the oxime group, a hydroxyl group was introduced as the active site. TBHA effectively enhanced the hydrophobicity and dispersion of BHA, while the other parameters were basically consistent. DOPA could effectively reduce the cost with stronger hydrophobicity. Therefore, based on

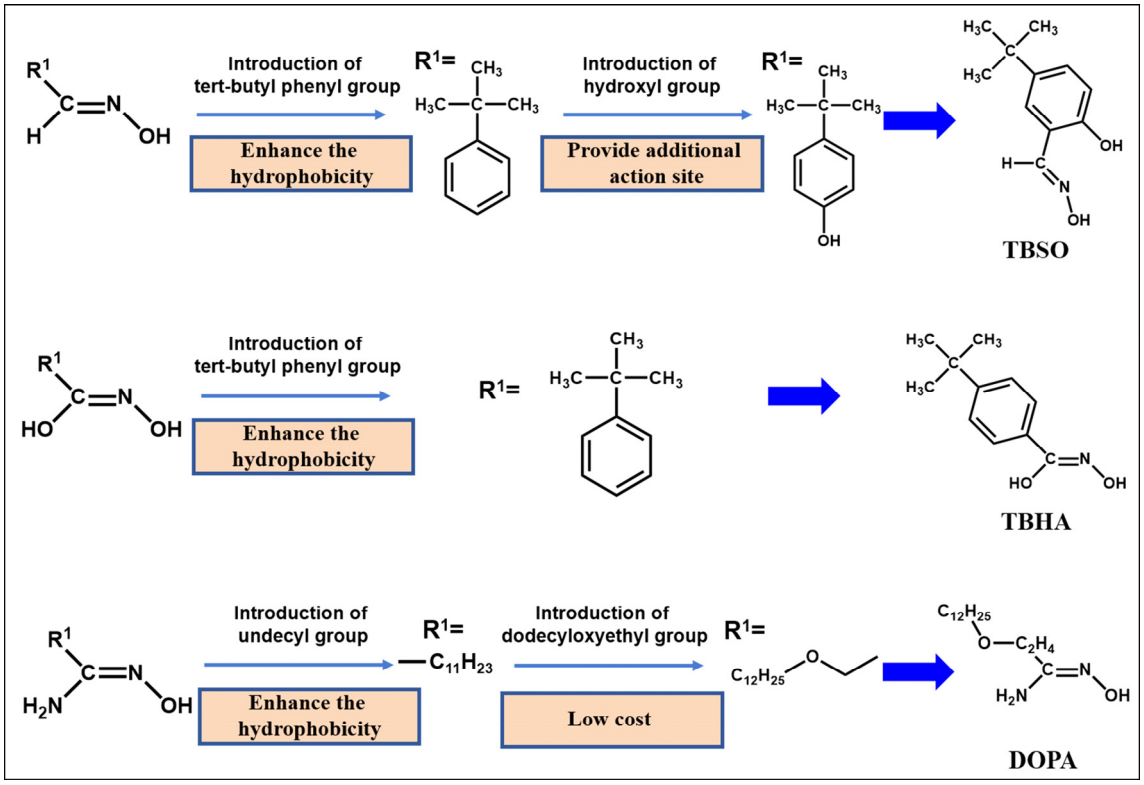

Fig. 6 Design flowchart of structurally modified oxime compounds

the DFT calculation analyses and corresponding structural modifications, three oxime compounds of TBSO, TBHA and DOPA were designed and should be considered as effective collectors in flotation.

To verify the flotation performances of TBSO, TBHA and DOPA, their flotation characteristics were investigated and are listed in Table 5. It was clear that TBSO and DOPA could achieve effective separation of malachite−quartz/calcite and wolframite−fluorite/calcite, respectively, which had superior flotation separation performances. However, TBHA only showed collecting ability to rhodochrosite, while its selection ability needs to be further investigated. Therefore, due to the wide study of BHA in cassiterite flotation, we used the performances of TBHA in cassiterite flotation to further examine and evaluate its flotation properties.

3.5 Flotation tests

Cassiterite is the most common mineral containing the vital metal tin, while flotation is considered as the crucial method for recovering fine cassiterite particles. To evaluate the flotation performances of TBHA and BHA for cassiterite and quartz, micro-flotation tests were conducted, and the results are exhibited in Fig. 7. In Fig. 7, the concentrations of TBHA and BHA were both 100 mg/L. As shown in Fig. 7(a), TBHA possessed a strong collecting ability for cassiterite over a wide pH range of 4.0−10.0, while the recovery of cassiterite was over 95.0% at pH 6.0. Unlike TBHA, BHA could only float approximately 40.0% cassiterite at pH 6.5−7.0, revealing its weak collecting ability to cassiterite. The collecting abilities of TBHA and BHA to quartz were both very weak, while the recoveries were all below 10.0%, revealing their good flotation separation effects. In Fig. 7(b), compared with BHA, TBHA could effectively float cassiterite at lower concentrations, which rendered it to be a superior collector in cassiterite flotation.

The results of bench-scale flotation tests are shown in Table 6. JSY-19 is a common industrial collector for cassiterite flotation and was produced by Hubei Jingjiang Flotation Reagents Co., Ltd., China. By using TBHA and JSY-19, the Sn grades in the rougher concentrates were 2.30% and 2.58%, respectively, suggesting that the selectivity of JSY-19 was better than TBHA. However, the Sn recovery in the rougher concentrates by using TBHA was significantly higher than that by using

Table 5 Characteristics of TBSO, DOPA and TBHA in flotation

Collector	Abbreviation	Characteristic	Ref.
5-tert-butylsalicylaldoxime	TBSO	Under alkaline conditions, malachite could be effectively separated from quartz and calcite by using 150 mg/L TBSO	[39]
3-dodecyloxy propyl amidoxime	DOPA	At pH 4.0−6.0, the effective separation of wolframite from calcium bearing minerals (fluorite and calcite) could be achieved by using 20 mg/L DOPA	[38]
4-tert-butylbenzohydroxamic acid (oxime)	TBHA	TBHA possesses strong collecting ability to rhodochrosite under alkaline conditions	[36]

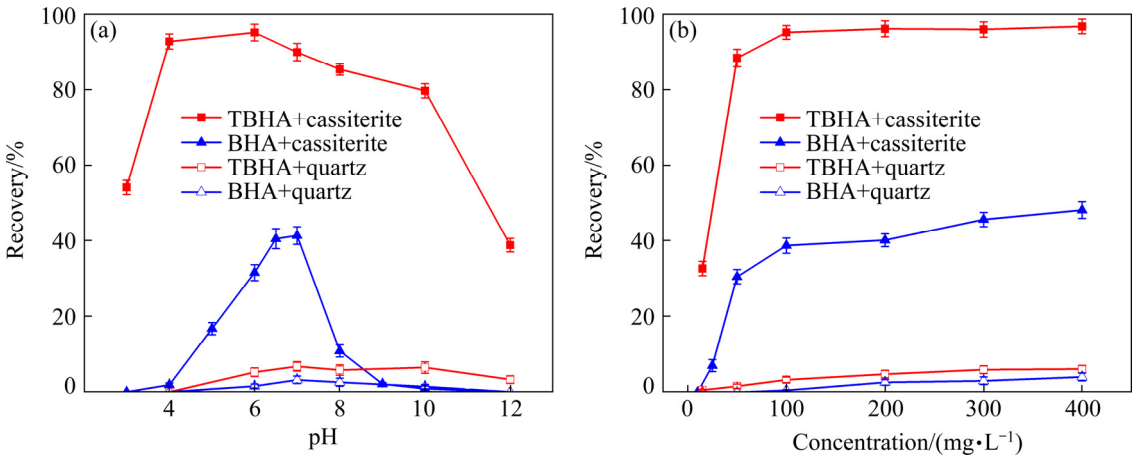

Fig. 7 Flotation recoveries of cassiterite and quartz as function of pH (a) and collector concentration (b)

Table 6 Results of bench-scale flotation tests

Collector	Concentration/(g·t^{-1})		Product	Mass fraction/%	Sn grade/%	Sn recovery/%
TBHA	Rougher	500	Tailings	4.84	2.30	60.25
	Cleaner	0	Concentrates	95.16	0.06	39.76
	Scavenger	0	Feed	100.00	0.17	100.00
JSY-19	Rougher	1500	Tailings	2.81	2.58	41.69
	Cleaner	150	Concentrates	97.19	0.10	58.31
	Scavenger	300	Feed	100.00	0.17	100.00

JSY-19, which revealed the strong collecting ability of TBHA to cassiterite. Moreover, the concentration of TBHA was obviously lower than that of JSY-19, while JSY-19 was toxic and environmentally harmful because it contained certain arsenic species. Therefore, TBHA was supposed to be an efficient collector in cassiterite flotation, which also proved the effectiveness of our previous structural modification to oxime compounds.

4 Conclusions

(1) The negative charges of oxime compounds were mainly concentrated on the nitrogen and oxygen atoms with lone pair electrons. Meanwhile, the four atoms of the oxime group in oxime compounds were basically in the same plane, leading to strong coordination ability with metal ions.

(2) In oxime compounds ($R^1R^2C{=}NOH$), the introduction of a phenyl group at the R^1 substituent group could improve the acidity of the compounds, while the nonpolar carbon chain (heptyl group) could effectively increase the hydrophobicity of the collector and benefit van der Waals interactions between the collector and mineral surfaces. Moreover, the introduction of a hydroxyl group at the R^2 substituent group could provide additional action sites to form stable chelates with metal ions, while the amino group could provide cationic sites to interact with negatively charged surfaces of minerals.

(3) TBSO could effectively separate malachite from quartz and calcite, DOPA could achieve the effective separation of wolframite from calcium-bearing minerals and TBHA was supposed to be an efficient collector in cassiterite flotation, which proved the effectiveness of our structural modification to oxime compounds.

Acknowledgments

The authors express their appreciation for the support of the National Natural Science Foundation of China (Nos. 51774329 and 51904337), and the High Performance Computing Center of Central South University, China.

References

[1] AHMADI A, REZAEI M, SADEGHIEH S M. Interaction effects of flotation reagents for SAG mill reject of copper sulphide ore using response surface methodology [J]. Transactions of Nonferrous Metals Society of China, 2021, 31: 792−806.

[2] GAO Zhi-yong, JIANG Zhe-yi, SUN Wei, GAO Yue-sheng. Typical roles of metal ions in mineral flotation: A review [J]. Transactions of Nonferrous Metals Society of China, 2021, 31: 2081−2101.

[3] BELKHETTAB I, BOUTAMINE S, SLAOUTI H, ZID M F, BOUGHZALA H, HANK Z. Synthesis, characterization and structural study of new vanadium complexes with phenolic oxime ligands [J]. Journal of Molecular Structure, 2020, 1206: 127597.

[4] ZHANG Ya-hui, LIU Qi, LI Li. Removal of iron from sythetic copper leach solution using a hydroxy-oxime chelating resin [J]. Hydrometallurgy, 2016, 164: 154−158.

[5] TIAN Gan, GENG Jun-xia, JIN Yong-dong, WANG Chun-li, LI Shu-qiong, CHEN Zhen, WANG Hang, ZHAO Yong-sheng, LI Shou-jian. Sorption of uranium(VI) using oxime-grafted ordered mesoporous carbon CMK-5 [J]. Journal of Hazardous Materials, 2011, 190: 442−450.

[6] WANG Li, HU Guang-yan, SUN Wei, KHOSO S A, LIU Run-qing, ZHANG Xiang-feng. Selective flotation of smithsonite from dolomite by using novel mixed collector system [J]. Transactions of Nonferrous Metals Society of China, 2019, 29: 1082−1089.

[7] WEI Zhao, SUN Wei, WANG Ping-shan, LIU Die, HAN Hai-sheng. A novel metal–organic complex surfactant for high-efficiency mineral flotation [J]. Chemical Engineering Journal, 2021, 426: 130853.

[8] WANG Cong, REN Shuai, SUN Wei, WU Si-hui, TAO Li-ming, DUAN Yao, WANG Jian-jun, GAO Zhi-yong. Selective flotation of scheelite from calcite using a novel self-assembled collector [J]. Minerals Engineering, 2021, 171: 107120.

[9] CAO Yang, SUN Lei, GAO Zhi-yong, SUN Wei, CAO Xue-feng. Activation mechanism of zinc ions in cassiterite flotation with benzohydroxamic acid as a collector [J]. Minerals Engineering, 2020, 156: 106523.

[10] LI Zhi-li, RAO Feng, SONG Shao-xian, URIBE-SALAS A, LÓPEZ-VALDIVIESO A. Effects of common ions on adsorption and flotation of malachite with salicylaldoxime [J]. Colloids and Surfaces A: Physicochemical and Engineering Aspects, 2019, 577: 421−428.

[11] HUANG Kai-hua, CAO Zhan-fang, WANG Shuai, YANG Jia, ZHONG Hong. Flotation performance and adsorption mechanism of styryl phosphonate mono-iso-octyl ester to malachite [J]. Colloids and Surfaces A: Physicochemical and Engineering Aspects, 2019, 579: 123698.

[12] HUANG Xiao-ping, HUANG Kai-hua, JIA Yun, WANG Shuai, CAO Zhan-fang, ZHONG Hong. Investigating the selectivity of a xanthate derivative for the flotation separation of chalcopyrite from pyrite [J]. Chemical Engineering Science, 2019, 205: 220−229.

[13] DENG Lan-qing, ZHAO Gang, ZHONG Hong, WANG Shuai, LIU Guang-yi. Investigation on the selectivity of N-((hydroxyamino)-alkyl) alkylamide surfactants for scheelite/calcite flotation separation [J]. Journal of Industrial and Engineering Chemistry, 2016, 33: 131−141.

[14] STASIAK J P, GRIGORYAN A, MURELLI R P. Spectrophotometric determination of α-hydroxytropolone p*K*a values: A structure-acidity relationship study [J]. Tetrahedron Letters, 2019, 60: 1643−1645.

[15] CHIRIȚĂ P, DUINEA M I, SÂRBU L G, BÎRSĂ L M, BAIBARAC M, SAVA F, MATEI E. Oxidation of chalcopyrite in air-equilibrated acidic solution: Inhibition with phenacyl derivatives [J]. Transactions of Nonferrous Metals Society of China, 2020, 30: 1928−1942.

[16] EL-LATEEF H M A, ELROUBY M. Synergistic inhibition effect of poly(ethylene glycol) and cetyltrimethylammonium bromide on corrosion of Zn and Zn−Ni alloys for alkaline batteries [J]. Transactions of Nonferrous Metals Society of China, 2020, 30: 259−274.

[17] KOKALJ A. On the alleged importance of the molecular electron-donating ability and the HOMO–LUMO gap in corrosion inhibition studies [J]. Corrosion Science, 2021, 180: 109016.

[18] ZHANG Hai-chang, LI Rui, DENG Zhi-feng, CUI Shuai-wei, WANG Yan-hui, ZHENG Meng, YANG Wen-jun. π-conjugated oligomers based on aminobenzodifuranone and diketopyrrolopyrrole [J]. Dyes and Pigments, 2020, 181: 108552.

[19] MARTINEZ J, AIELLO I, BELLUSCI A, CRISPINI A, GHEDINI M. Tetranuclear zinc complexes of ligands containing the 2-pyridyl oxime chelating site [J]. Inorganica Chimica Acta, 2008, 361: 2677−2682.

[20] YANG Xiang-lin, LIU Sheng, LIU Guang-yi, ZHONG Hong. A DFT study on the structure–reactivity relationship of aliphatic oxime derivatives as copper chelating agents and malachite flotation collectors [J]. Journal of Industrial and Engineering Chemistry, 2017, 46: 404−415.

[21] BALACHANDRAN V, NATARAJ A, KARTHICK T. Molecular structure, spectroscopic (FT-IR, FT-Raman) studies and first-order molecular hyperpolarizabilities, HOMO−LUMO, NBO analysis of 2-hydroxy-*p*-toluic acid [J]. Spectrochimica Acta (Part A): Molecular and Biomolecular Spectroscopy, 2013, 104: 114−129.

[22] HAN Gui-hong, DU Yi-fan, HUANG Yan-fang, YANG Shu-zhen, WANG Wen-juan, SU Sheng-peng, LIU Bing-bing. Efficient removal of hazardous benzohydroxamic acid (BHA) contaminants from the industrial beneficiation wastewaters by facile precipitation flotation process [J]. Separation and Purification Technology, 2021, 279: 119718.

[23] ZHANG Xia, DU Hao, WANG Xu-ming, MILLER J D. Surface chemistry aspects of bastnaesite flotation with octyl hydroxamate [J]. International Journal of Mineral Processing, 2014, 133: 29−38.

[24] YANG Xiu-li, AI Guang-hua. Effects of surface electrical property and solution chemistry on fine wolframite flotation [J]. Separation and Purification Technology, 2016, 170: 272−279.

[25] CHEN Chen, SUN Wei, ZHU Hai-ling, LIU Run-qin. A novel green depressant for flotation separation of scheelite from calcite [J]. Transactions of Nonferrous Metals Society of China, 2021, 31: 2493−2500.

[26] MARION C, JORDENS A, LI Rong-hao, RUDOLPH M, WATERS K E. An evaluation of hydroxamate collectors for malachite flotation [J]. Separation and Purification Technology, 2017, 183: 258−269.

[27] BUCKLEY A N, PARKER G K. Adsorption of *n*-octanohydroxamate collector on iron oxides [J]. International Journal of Mineral Processing, 2013, 121: 70−89.

[28] ACKERMAN P K, HARRIS G H, KLIMPEL R R, APLAN F F. Use of chelating agents as collectors in the flotation of copper sulfides and pyrite [J]. Mining, Metallurgy & Exploration, 1999, 16: 27−35.

[29] REN Liu-yi, QIU Hang, ZHANG Ming, FENG Kai-yue, LIU Peng, GUO Jing, FENG Jian. Behavior of lead ions in cassiterite flotation using octanohydroxamic acid [J]. Industrial & Engineering Chemistry Research, 2017, 56: 8723−8728.

[30] LIU Sheng, XIE Lei, LIU Jun, LIU Guang-yi, ZHONG Hong, WANG Yi-xiang, ZENG Hong-bo. Probing the interactions of hydroxamic acid and mineral surfaces: Molecular mechanism underlying the selective separation [J]. Chemical Engineering Journal, 2019, 374: 123−132.

[31] LIU Sheng, LIU Guang-yi, HUANG Yao-guo, ZHONG Hong. Hydrophobic intensification flotation: Comparison of collector containing two minerophilic groups with conventional collectors [J]. Transactions of Nonferrous Metals Society of China, 2020, 30: 2536−2546.

[32] LU Yu-xi, WANG Shuai, ZHONG Hong. Study on the role of a hydroxamic acid derivative in wolframite flotation: Selective separation and adsorption mechanism [J]. Applied Surface Science, 2021, 550: 149223.

[33] GIBSON C E, HANSULD R, KELEBEK S, AGHAMIRIAN M. Behaviour of ilmenite as a gangue mineral in the benzohydroxamic flotation of a complex pyrochlore-bearing ore [J]. Minerals Engineering, 2017, 109: 98−108.

[34] SUN Lei, HU Yue-hua, SUN Wei. Effect and mechanism of octanol in cassiterite flotation using benzohydroxamic acid

as collector [J]. Transactions of Nonferrous Metals Society of China, 2016, 26: 3253−3257.

[35] JIANG Yu-ren, XUE Yu-lan. Synthesis and collecting activity of methyl benzamidoxime [J]. Journal of Basic Science and Engineering, 2000, 3: 230−235.

[36] ZHAO Gang, DAI Ting, WANG Shuai, ZHONG Hong. Study on a novel hydroxamic acid as the collector of rhodochrosite [J]. Physicochemical Problems of Mineral Processing, 2018, 54: 423−439.

[37] FAN Gui-xia, ZHANG Meng-yun, PENG Wei-jun, ZHOU Guo-li, DENG Li-jun, CHANG Lu-ping, CAO Yi-jun, LI Peng. Clean products from coal gasification waste by flotation using waste engine oil as collector: Synergetic cleaner disposal of wastes [J]. Journal of Cleaner Production, 2021, 286: 124943.

[38] LU Yu-xi, WANG Shuai, ZHONG Hong. New insights into separating wolframite from calcium bearing minerals by flotation [J]. Journal of Industrial and Engineering Chemistry, 2021, 97: 549−559.

[39] LI Li-qing, ZHAO Jing-hua, XIAO Yan-yin, HUANG Zhi-qiang, GUO Zhi-zhong, LI Fang-xu, DENG Lan-qing. Flotation performance and adsorption mechanism of malachite with tert-butylsalicylaldoxime [J]. Separation and Purification Technology, 2019, 210: 843−849.

基于 DFT 计算的肟类浮选捕收剂的构效关系

卢宇熙，王 帅，曹占芳，马 鑫，钟 宏

中南大学 化学化工学院 锰资源高效清洁利用湖南省重点实验室，长沙 410083

摘 要：研究不同取代基的肟类化合物(R^1R^2C═NOH，其中 R^1/R^2 为烷基)的结构与其相应浮选性能之间的关系。密度泛函理论(DFT)计算结果表明，在 R^1 位置引入苯基可以提高捕收剂分子的酸性，而引入庚基可以有效地提高其疏水性，有利于强化范德华相互作用。同时，在 R^2 位置引入的氨基可以提供阳离子位点，并与矿物的负电荷表面相互作用，而引入的羟基可以提供与金属离子形成稳定螯合物的额外作用位点。根据构效关系进行结构优化，筛选得到 3 种高效捕收剂。这 3 种捕收剂都具有优异的浮选分离性能，证明本文作者对肟类化合物进行结构改性的有效性。

关键词：肟类化合物；浮选捕收剂；DFT 计算；构效关系；结构改性

(Edited by Wei-ping CHEN)